BJR, 2026, **99**, 122–132
https://doi.org/10.1093/bjr/tqaf231
Advance access publication: 16 September 2025
Research Article

Ultrasound imaging/guidance for insertional Achilles tendinopathy

Vincenzo Ricci, MD*[,1], Toru Omodani, MD[2], Ke-Vin Chang, MD, PhD[3], Costantino Ricci, MD, PhD[4], Ondřej Naňka, MD, PhD*[,5], Antonio Corvino, MD, PhD[6], Massimo Caulo, MD, PhD[7], Andrea Delli Pizzi, MD, PhD[8,9], Vito Cantisani, MD, PhD[10], Giorgio Tamborrini, MD[11,12], Giulio Cocco, MD, PhD[#,7], Levent Özçakar, MD[#,13]

[1]Physical and Rehabilitation Medicine Unit, Luigi Sacco University Hospital, Milan 20157, Italy
[2]Orthopaedics, Tokyo Advanced Orthopaedics, Tokyo 182-0033, Japan
[3]Department of Physical Medicine and Rehabilitation and Community and Geriatric Research Center, National Taiwan University Hospital, Taipei 100, Taiwan
[4]Department of Medical and Surgical Sciences (DIMEC), University of Bologna, Bologna 40126, Italy
[5]Institute of Anatomy, First Faculty of Medicine, Charles University, Prague 12800, Czech Republic
[6]Medical, Movement and Wellbeing Sciences Department, University of Naples "Parthenope", Naples 80133, Italy
[7]Department of Neuroscience, Imaging and Clinical Sciences, G. d'Annunzio University, Chieti 66100, Italy
[8]Department of Innovative Technologies in Medicine and Dentistry, G. d'Annunzio University, Chieti 66100, Italy
[9]ITAB Institute for Advanced Biomedical Technologies, G. d'Annunzio University, Chieti 66100, Italy
[10]Department of Radiological, Oncological and Anatomopathological Sciences, Sapienza, University of Rome, Rome 00185, Italy
[11]UZR, Ultraschallzentrum und Institut für Rheumatologie, Basel 4051, Switzerland
[12]Rheumatology Clinic, University Hospital of Basel, Basel 4031, Switzerland
[13]Department of Physical and Rehabilitation Medicine, Hacettepe University Medical School, Ankara 06230, Turkey

*Corresponding authors: Ondřej Naňka, MD, PhD, Institute of Anatomy, First Faculty of Medicine, Charles University, U Nemocnice 3, 12800 Prague, Czech Republic (ondrej.nanka@lf1.cuni.cz) and Vincenzo Ricci, MD, Physical and Rehabilitation Medicine Unit, Luigi Sacco University Hospital, ASST Fatebenefratelli-Sacco, Via Giovanni Battista Grassi, 74, 20157 Milan, Italy (ricci.vincenzo@asst-fbf-sacco.it)

#Giulio Cocco and Levent Özçakar contributed equally to this work and shared the senior authorship.

Abstract

Objectives: This observational study aimed to define a standardized sonographic approach for evaluating the elementary lesions of the tendon-bone junction (TBJ) in insertional Achilles tendinopathy (IAT).

Methods: Using high-frequency transducers, we matched the histological microarchitecture and the anatomical features of the TBJ of the Achilles tendon in patients with a clinical diagnosis of IAT. Colour/power Doppler assessments have been performed as well.

Results: Fifty-eight patients, with a mean age of 54 years (54.50 ± 11.72) and a gender distribution of 32 males (55.17%) and 26 females (44.83%), were enrolled in this observational study. Five elementary lesions of IAT were sonographically defined: bone spur, calcified longitudinal fissuration, intra-tendinous bony formation, tendon-bone disjunction, and fibrocartilage hyperemia. Moreover, specific sonographic signs have been identified to differentiate bony spurs in the growing phase and end-stage.

Conclusions: Using high-frequency B-mode and high-sensitive Doppler imaging, detailed sonographic assessment of the TBJ can be performed in IAT patients. The aforementioned 5 elementary lesions can be considered as a standardized approach for prompt examination of this complex/anatomical region.

Advances in knowledge: Recent advances in ultrasound equipment allow for accurate assessment of the TBJ of the AT. The present observational study defined 5 elementary sonographic lesions of the IAT as bone spur, calcified longitudinal fissuration, intra-tendinous bony formation, tendon-bone disjunction, and fibrocartilage hyperemia. Pertinent ultrasound-guided procedures targeting the TBJ are also discussed.

Keywords: ankle; enthesis; tendon; fibrocartilage; calcification; sonography; Doppler.

Background

Insertional Achilles tendinopathy (IAT) commonly refers to pain and swelling at the calcaneal attachment of the Achilles tendon (AT).[1,2] At this specific anatomical region, the entheseal anchorage network of the AT comprises a tendon-bone junction (TBJ) coupled with the deep retrocalcaneal bursa, the posteroinferior wedge of the Kager's fat pad deeply, and the subcutaneous (pre-Achilles) calcaneal bursae superficially.[3,4] In the pertinent literature, the sonographic appearance of the tendon-bone interface is oftentimes described as a double-layer structure, that is, superficial hypoechoic band representing as the (fibro)cartilage and a deep hyperechoic line as the cortical bone.[5,6] The histological/anatomical changes involving the enthesis in IAT patients often encompass a wide spectrum of sonographic findings not reported in the previous definitions—confined more to inflammatory diseases.[7,8]

To this end, the main goal of the present observational study was to comprehensively describe and illustrate the

Received: 11 February 2025; **Revised:** 8 August 2025; **Accepted:** 5 September 2025

mechanical/degenerative lesions of the TBJ in IAT patients. Starting from the histological and anatomical features, and using high-frequency transducers, we proposed a standardized sonographic protocol which can serve as a ready-to-use guide in daily practice.

Methods

This observational investigation involved patients with a clinical diagnosis of IAT who were referred to our department for ultrasound (US) examination between June 2024 and December 2024. The inclusion criteria were the presence of tenderness/swelling at the insertion of AT for at least 4-6 months and age of at least 18 years, and radiographic absence of any fracture of the calcaneal bone (in the last 30 days). Previous trauma, injection or surgery of the ankle or hindfoot and any rheumatic or endocrine problem involving the AT were defined as exclusion criteria.

Written permission was obtained from each and every patient before sonographic images/videos were acquired. No ethical committee was involved in the present study because all the pictures of the anatomical specimens were elaborated using donated bodies—with the courtesy of the Institute of Anatomy, First Faculty of Medicine, Charles University, Prague. Likewise, all the histological specimens were elaborated with the courtesy of the DIAP-Dipartimento InterAziendale di Anatomia Patologica di Bologna, Maggiore Hospital-AUSL Bologna, Italy; and the Department of Medical and Surgical Sciences (DIMEC), University of Bologna, Italy.

To propose a standardized assessment and to define the sonographic elementary lesions in IAT patients, the authors:

1) reviewed the literature to define the histological layers and the anatomical surfaces of the calcaneal tuberosity (ie, calcaneal facets) to be assessed during the US examination
2) described the histopathological findings of the IAT (ie, elementary lesions) to define exactly what to characterize/assess during the US assessment
3) performed multiple US examinations in IAT patients to describe the elementary lesions of the TBJ of the AT.

The images/videos have been acquired using i18LX5 high-frequency transducer, Canon Aplio I800/I700, Canon Medical Systems, Shimoishigami, Otawara-Shi, Japan. During the US examination, the patients were lying prone, with the ankle joint in a neutral position and the foot hanging over the edge of the examination bed. A large amount of gel between the US transducer and the heel skin has been used to avoid unintentional compression of the superficial soft tissues—that wrap the posterior surface of the calcaneus—preserving the native shape of the different histological layers. The transducer was positioned in the longitudinal plane, covering the distal portion of the AT and the entire surface of the calcaneal tuberosity (superior, middle, and inferior facets). To assess the entire width of the retrocalcaneal space, the authors have used at least 3 sagittal views as follows: (the probe being) on the midline, medial parasagittal, and lateral parasagittal planes. Then, rotating the transducer 90°, multiple transverse scans of the calcaneal tuberosity were acquired at the levels of different calcaneal facets.

Results and discussion

Histology

This is a fibrocartilaginous transitional zone (TZ) connecting the tendon fibres to the calcaneal cortex (Figure 1). The fibrocartilage contains rows of rounded cells surrounded by a metachromatic pericellular matrix and separated by parallel arrays of collagen fibres.[9] A tridimensional mixture of type II-III collagen fibres coupled with proteoglycans presents a network-like spatial arrangement.[10] Due to their negative charge, proteoglycans—localized in the interstices between the collagen fibres—provide a swelling pressure within the fibrocartilage that counteracts compressive mechanical stresses.[11,12] Additionally, small leucine-rich proteoglycans modulate fibre sliding properties and viscoelastic features of the TBJ.[13,14]

There are 3 main/characteristic histopathological changes of the TBJ in IAT patients: (1) bone spurs (BSs), (2) longitudinal fissurations, and (3) transverse tears.[9,15,16] Spurs are projections of bone tissue extending from the middle/inferior facet of the calcaneal tuberosity into the tendon tissue—surrounded by an external coat of metachromatic extracellular matrix and (fibro)cartilage tissue.[9,15,16] Indeed, tendon fibroblasts switch into fibrocartilage cells arranged in rows (metaplastic process) that reabsorb themselves and generate space for neocapillaries stemming from the bone marrow. After the vascular invasion, new bone tissue is deposited along the inner walls of the intra-tendinous tunnels and the spur is formed.[15,16]

Longitudinal fissurations are splits of the fibrocartilage containing amorphous metachromatic material, poorly organized fibrous extracellular matrix, and some clusters of cells along the inner edges.[9] They can progressively ossify, becoming visible on X-ray as linear/lamellar calcifications bridging the cortical bone of the calcaneus and more distal tendon fibres.[9,15,16] In this sense, calcified longitudinal fissures may "mimic" spurs on radiographs but do not contain any bone cell/matrix.[15] Lastly, transverse tears are micro-cracks of the fibrocartilage, filled with fat cells and vascular connective tissue—without cell clusters.[9,15,16]

Anatomy

There are 3 (superior, middle, and inferior) facets on the posterior surface of the calcaneal tuberosity (Figure 2). The superior facet is covered by periosteal fibrocartilage that histologically corresponds to the anterior wall of the deep retrocalcaneal bursa—without any tendon fibres attached at this level.[17-19] The middle and inferior facets form the anatomical footprint of the AT (fAT), where a fibrocartilaginous layer is interposed between the tendon and the bone (Figure 3). Deep fibres of the AT originating from the soleus muscle attach to the medial aspect of the middle facet. Instead, tendon fascicles originating from the lateral head of the gastrocnemius muscle insert on the lateral aspect of the middle facet.[17-20] Likewise, the superficial fibres of the AT originating from the medial head of the gastrocnemius muscle attach over the entire width of the inferior facet of the calcaneal tuberosity—presenting a histological continuum with the plantar fascia via the periosteum of the calcaneus.[17-20] As such, the AT, plantar fascia, calcaneal periosteum, and cortex of the calcaneal tuberosity can be considered a unique anatomical and functional unit of the hindfoot.[21,22] The tendon presents a crescent-shaped insertion on the middle/inferior facet of the calcaneal tuberosity, with medial and lateral extensions.[23,24] The medial extensions are more prominent

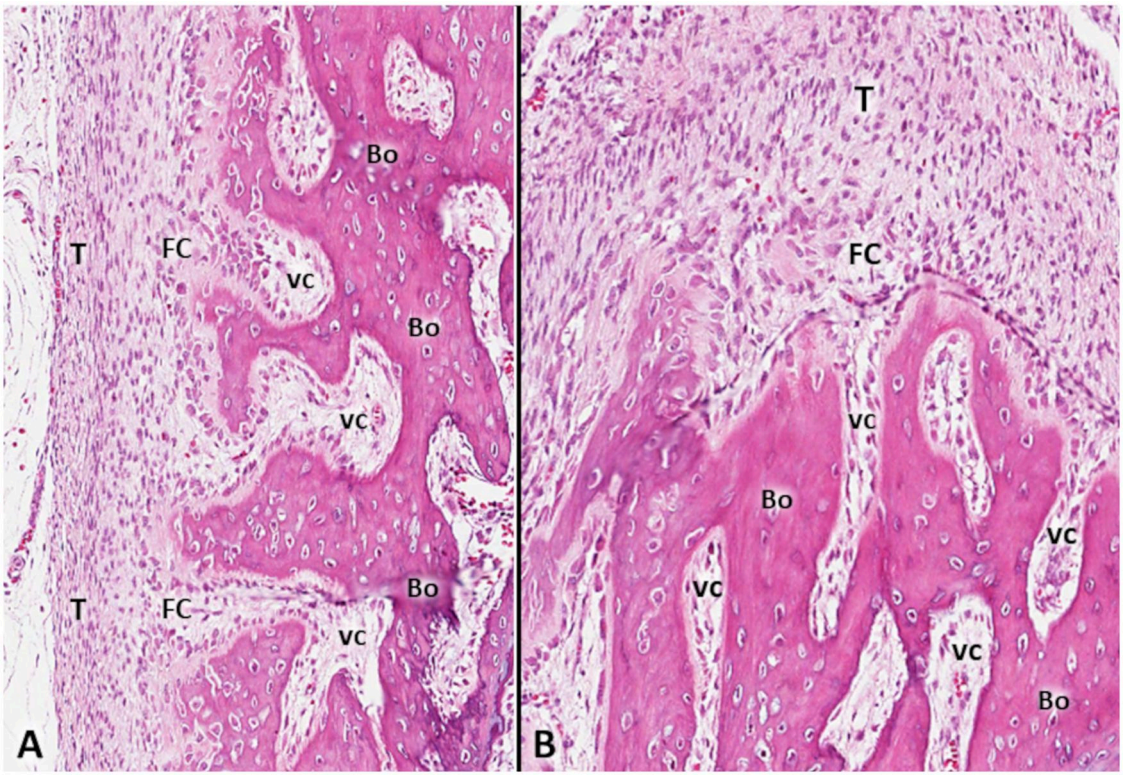

Figure 1. The fibrocartilaginous plate (FC)—composed of a mixture of immature, epithelioid round chondrocytes and fibroblasts embedded in a myxoid matrix—undergoing an endochondral ossification to form the underlying bony scaffold (Bo) composed of lamellar bone tissue with inner osteoblast and osteoclast units (A). Multiple vascular channels (VC) crossing the bone marrow and reaching the fibrocartilage can be observed (B). Histological transition from the FC to the overlying tendon tissue (T) is marked by the disappearance of chondrocytes, and by the abrupt change in fibroblasts' density and spatial arrangement that increases in the number and acquires a densely-packed fascicular pattern (A, B) (hematoxylin & eosin, original magnification ×180, endochondral ossification unit sampled from a fetus at term).

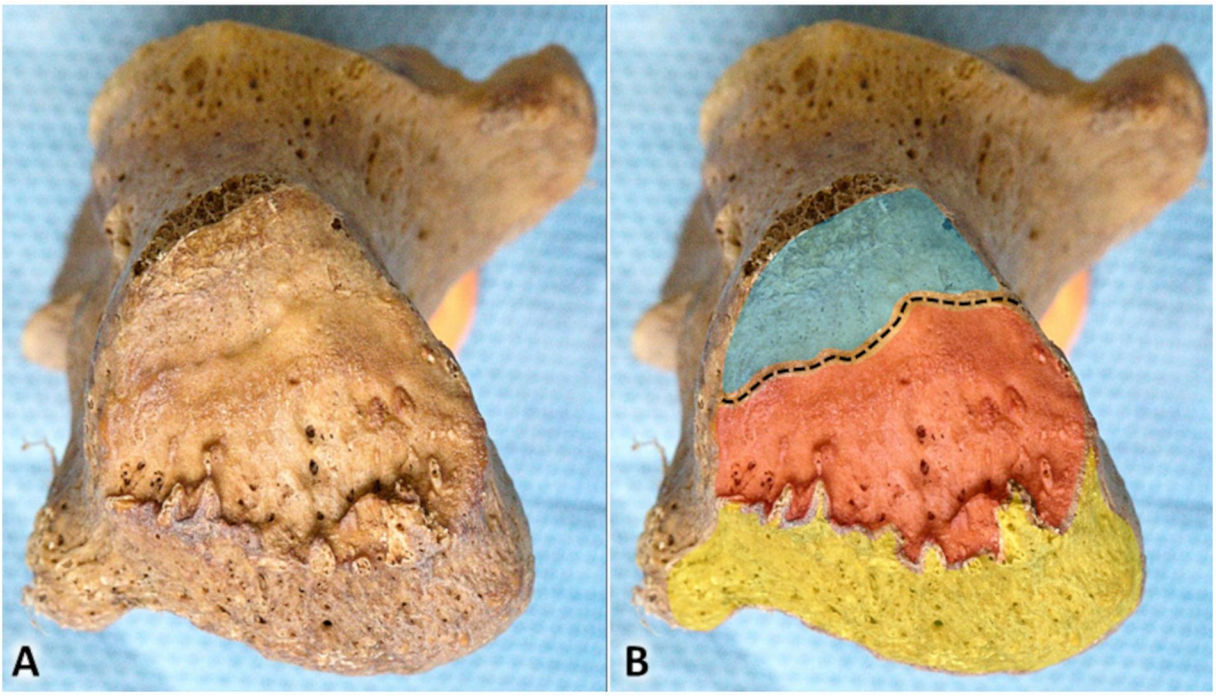

Figure 2. The transitional zone (*black dotted line*) is a small bony groove on the calcaneal tuberosity dividing the superior facet (*light blue*) from the middle/inferior facet (*light red*) (A, B). More distally, the bone surface of the calcaneum is covered by periosteum (*light yellow*).

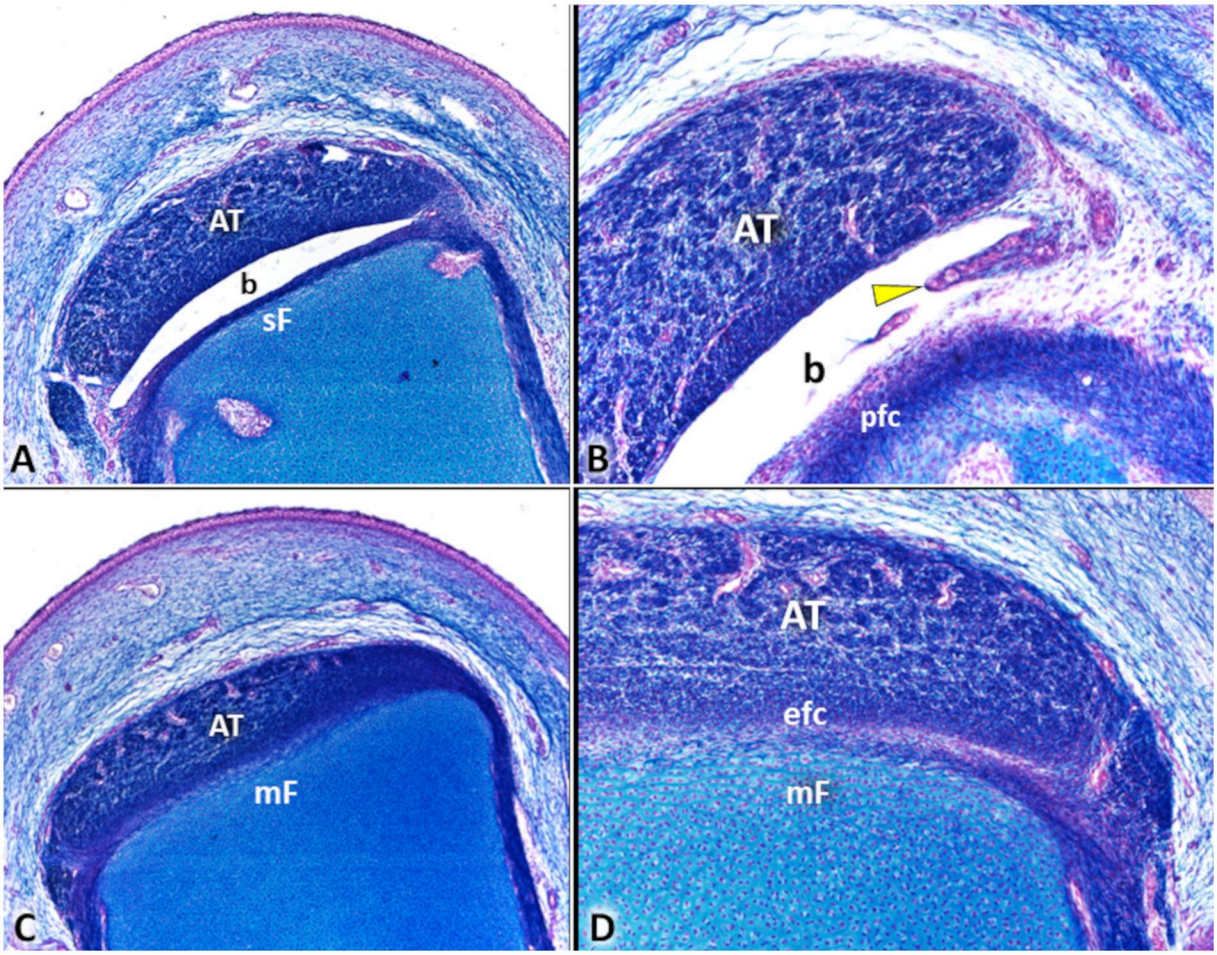

Figure 3. The superior facet (sF) of the calcaneal tuberosity is covered by periosteal fibrocartilage (pfc) that anatomically represents the anterior wall of the deep retrocalcaneal bursa (b) (A, B). The Achilles tendon (AT) attaches to the middle facet (mF) of the calcaneal tuberosity through the enthesial fibrocartilage (efc) (C, D). Yellow arrowhead: synovial plica of the deep retrocalcaneal bursa (87-day human fetus, staining Mayer's hematoxylin & eosin + alcian blue).

than the lateral ones, with maximum dimensions of 9.1 mm (medial) and 5.5 mm (lateral).[23,24] The width of the tendon's insertion footprint varies between 20 and 48 mm among individuals.[17,25]

Between the AT and the superficial retrocalcaneal fat pad, superficial synovial bursae and cutaneous nerves reside within a gliding layer of loose connective tissue.[26] Moreover, tiny vascular elements originating from larger donator vessels (located in the loose connective tissue) penetrate the posterior surface of the AT, feeding the superficial tendon fibres (Figure 4).

Study cohort and US imaging

From an initial group of 64 patients, 4 were excluded due to age (<18 years) and 2 due to previous surgery. The study cohort, therefore, consisted of 58 patients, with a mean age of 54 years (54.50 ± 11.72). The gender distribution was 32 males (55.17%) and 26 females (44.83%). Matching the anatomical/histopathological features with the sonographic patterns of the 58 IAT patients, 5 elementary lesions were defined (Table 1). Bone spur, calcified longitudinal fissuration (CLF), intra-tendinous bone formation (ITBF), tendon-bone disjunction (TBD), and fibrocartilage hyperemia (FCH).

Bone spur

Positioning the transducer in the longitudinal plane, the superior facet of the calcaneal tuberosity can accurately/normally be differentiated from the anatomical fAT, corresponding to the middle and inferior facets. A small bony groove known as the TZ of the calcaneal tuberosity can be visualized between them (Figure 5). This anatomical landmark, indicating the passage from the superior to the middle facet, has been defined as a *shallow groove*.[26,27]

Bony overgrowth of the middle facet leads to progressive disappearance of the TZ of the calcaneal tuberosity, with the typical sonographic pattern of the white bump.[28,29] The tendon fibres pass over the superior facet and directly attach to the hyperechoic BS, losing their most distal portion's triangular shape (Figure 5).[30] In some patients, the hyperechoic bump of the BS can be covered by a hypoechoic layer, representing a cartilaginous coat related to the active growth of the bone formation.[31] The cartilaginous envelope can be homogeneously hypoechoic or may present some inner hyperechoic spots, due to focal metaplasia of the cartilage into bone (Figure 5).

In the very early phase, the BS is largely cartilaginous (due to incomplete ossification) and presents an atypical sonographic pattern (Video S1). It appears as thick hypoechoic

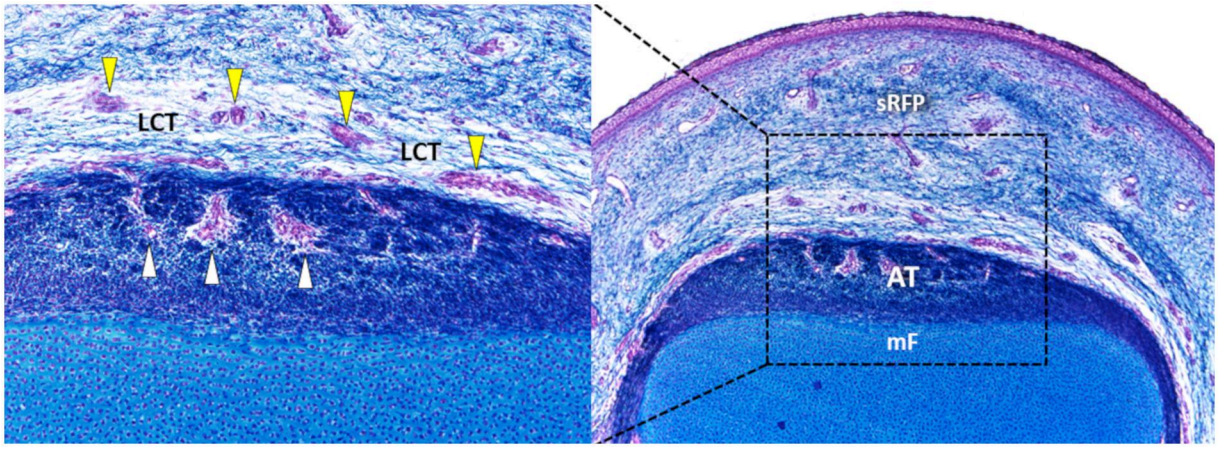

Figure 4. A gliding layer of loose connective tissue (LCT) is located between the superficial retrocalcaneal fat pad (sRFP) and the Achilles tendon (AT). The vascular network shows larger donator vessels (yellow arrowheads) between the tendon and the fat tissue, and smaller penetrating vessels (white arrowheads) that cross the posterior surface of the tendon feeding its superficial fibres (87-day human fetus, staining Mayer's hematoxylin & eosin + alcian blue).

Table 1. Suggested US examination protocol.

US finding	Technical note
BS	Typical pattern: hyperechoic bump of middle/inferior facet of the calcaneal tuberosity with disappearance of the transitional zone Atypical pattern[a]: hyperechoic bump with hypoechoic (cartilaginous) coat, hypoechoic cartilaginous laminae +/– hypervascularization, finger-shaped formation with hyperechoic bony coat and hypoechoic cartilaginous core
CLF	a thin hyperechoic line without posterior acoustic shadowing—connecting the middle/inferior facet of the calcaneal tuberosity to the tendon
ITBF	Hyperechoic regular-in-shape bony fragment embedded within the tendon tissue with complete posterior acoustic shadowing *(differential diagnosis with bony loose body)*
TBD	Focal hypo/anechoic gap involving the tendon-bone interface with retraction of the proximal stump (*superficial vs. deep tendon fibers*[b])
FCH	Early phase: globular vascular pattern in the most distal portion of the TBJ Advanced phase: vertically oriented vessels within the FC (*donator vessels*), horizontally oriented vessels bridging the FC and the tendon (*penetrating vessels*)

Abbreviations: BS = bone spur; CLF = calcified longitudinal fissuration; FCH = fibrocartilage hyperemia; ITBF = intra-tendinous bony formation; TBJ = tendon-bone disjunction.
[a]Mainly related to bone spurs in the growing phase.
[b]US-guided dilatation of the deep retrocalcaneal bursa to optimize sonographic visibility of the TBD involving the deep tendon fibres.

laminae connecting the middle/inferior facet of the calcaneal tuberosity and the AT (Figure 6). Rotating the probe 90°, transverse scans accurately confirm the presence of hypo/anechoic cartilage tissue in between the hyperechoic cortical bone of the calcaneal facets and the tendon tissue (Figure 7). Sono-compression with the transducer and dynamic US scans with active/passive foot movements are useful additional diagnostic techniques to differentiate between cartilaginous laminae of a developing BS and focal tendon injuries.[32,33] Colour/power Doppler usually shows rich hypervascularization of the cartilaginous spurs (Figure 6, Video S2)—due to invasion by penetrating vessels originating from the vascular channels of bone marrow (Figure 1). Progressive deposition of bone tissue along the outer edges of the cartilaginous spur can be sonographically visualized as a hyperechoic envelope surrounding the hypoechoic core of the "osteocartilaginous" formation—ie, a finger-shaped pattern (Figure 6, Video S3).

Lastly, abnormal friction between the retrocalcaneal fat pad and the underlying BS may progressively lead to synovial hypertrophy of the superficial retrocalcaneal (pre-Achilles) bursae.[26] Superficial retrocalcaneal bursitis usually presents as a small hypoechoic nodular mass, unlike the surrounding tubular-shaped vessels (Figure 8).[26] Sono-palpation can be performed to differentiate between the hardly compressible and painful hypertrophic pre-Achilles bursitis and the easily compressible/painless superficial retrocalcaneal veins (Video S4). Colour/power Doppler can also be used to distinguish the venous flow signals from the hypertrophic superficial retrocalcaneal bursitis that commonly does not show hyperemia/hypervascularization (Figure 8).

Calcified longitudinal fissuration

Longitudinal cracks of the TBJ of the AT may progressively develop calcifying phenomena—generating a sonographic pattern with thin hyperechoic lines connecting the tendon to the middle/inferior facet of the calcaneal tuberosity (Figure 9).[9,15,16] The CLF does not present posterior acoustic shadowing as the BS or the intra-tendinous calcification, but it allows the US beam to penetrate the deeper tissues (Video S5).[34] Therefore, sonographic visualization of the underlying middle/inferior facet is commonly preserved both in longitudinal and transverse scans (Video S6).

The CLF is aligned with the tendon fibres and does not lead to thickening or disruption of the tendon shape. It may be coupled with other sonographic findings such as the deep retrocalcaneal exudative bursitis and the BS; however, in early disease phases, it can also be visualized (as a unique/single sonographic abnormality).[30]

Intra-tendinous bone formation

Due to the metaplasia of tendon fibroblasts, tendon tissue may convert into cartilage tissue in the early phase and into bone tissue in more advanced stages of the disease.[9,15,16] The ITBF displays the typical sonographic pattern of bone,

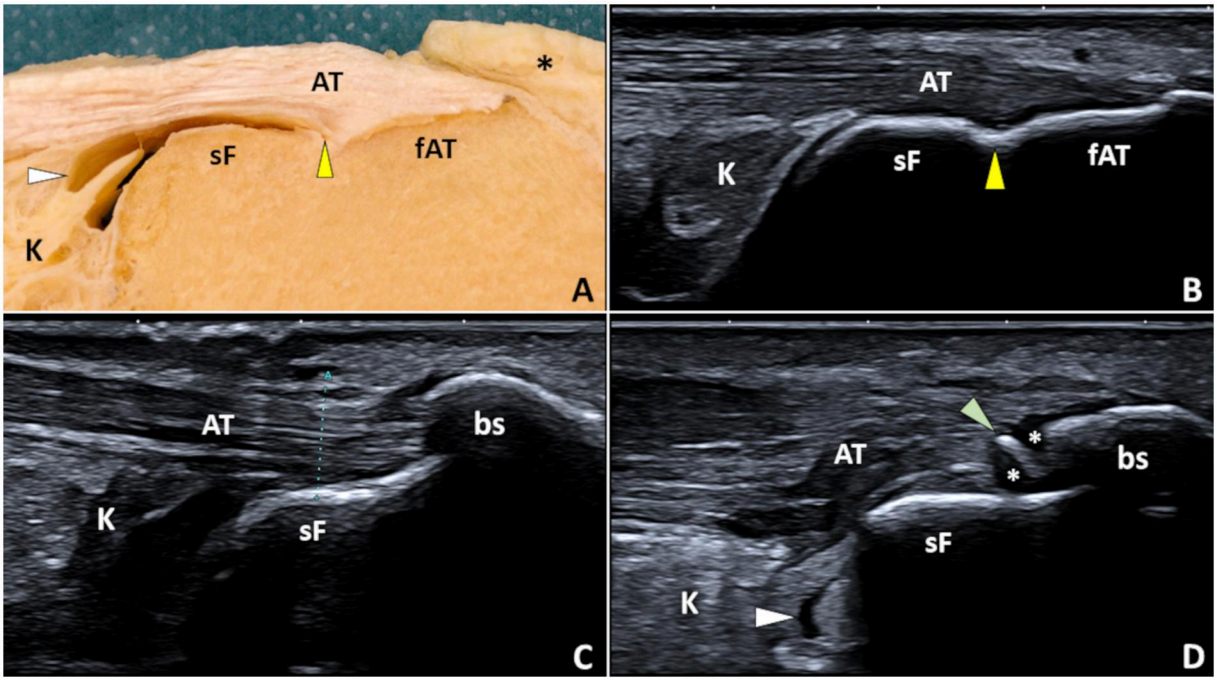

Figure 5. Cadaveric sample (A) and high-resolution ultrasound image (B) show normal Kager's fat pad (K) and the transitional zone (yellow arrowhead) from the superior facet (sF) of the calcaneal tuberosity to the footprint of the Achilles tendon (fAT). In pathological conditions (C), the bony spur (bs) hides the transitional zone of the calcaneal tuberosity with the disappearance of the triangular-shaped distal portion of the Achilles tendon (AT). In some patients (D), the developing bony spur (bs) may be covered by a hypoechoic cartilaginous coat (white asterisks) with inner lamellar bone depositions (green arrowhead). White arrowhead: deep retrocalcaneal bursa.

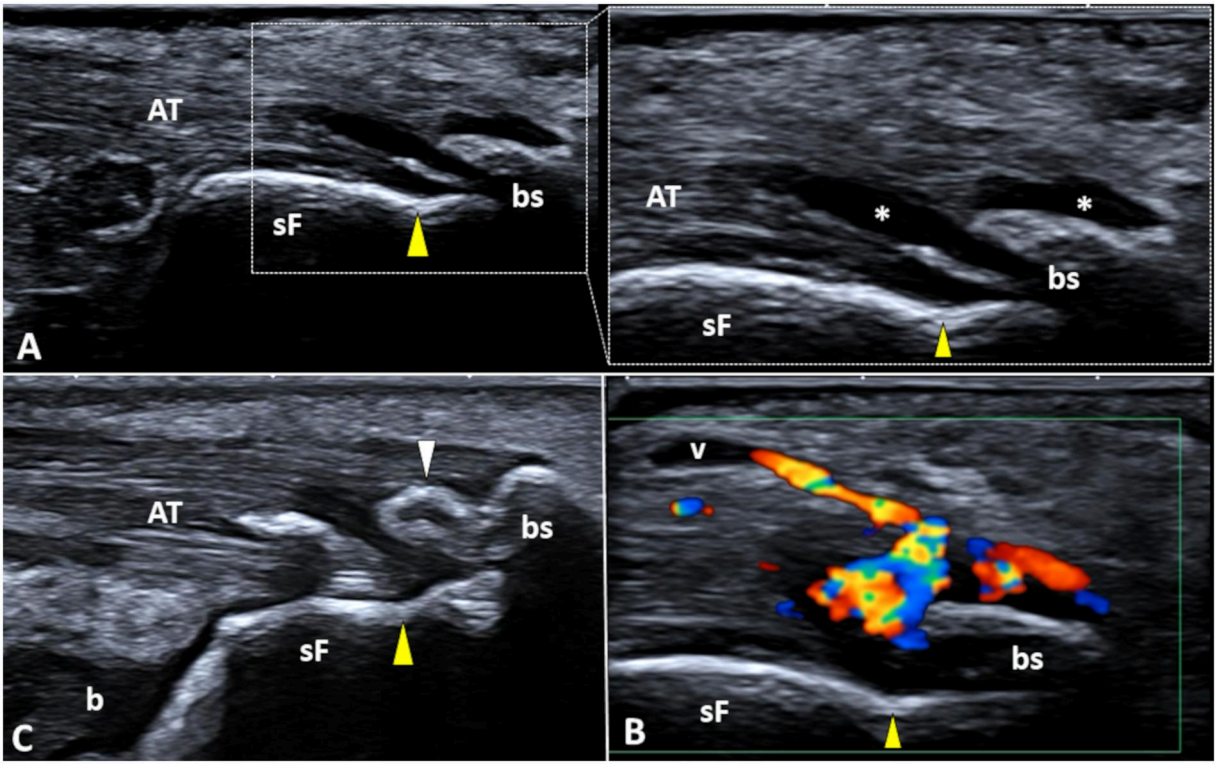

Figure 6. In the early phase of endochondral ossification (A), the transitional zone (*yellow arrowhead*) of the calcaneal tuberosity between the superior facet (*sF*) and the developing bony spur (*bs*) is still preserved and hypoechoic cartilaginous laminae (*white asterisks*) can be visualized insinuating between the tendon fibres. Colour Doppler shows the perfusion pattern of the cartilage spurs due to vascular invasion from the bone marrow channels (B). Progressive ossification of the outer walls of the cartilaginous spur can be observed as a thin hyperechoic coat, covering the inner hypoechoic cartilage tissue (*white arrowhead*), that is, the "osteocartilaginous finger" of the tendon-bone junction (C). Black asterisk: superficial retrocalcaneal fat pad. Abbreviations: AT = Achilles tendon; b = deep retrocalcaneal bursa.

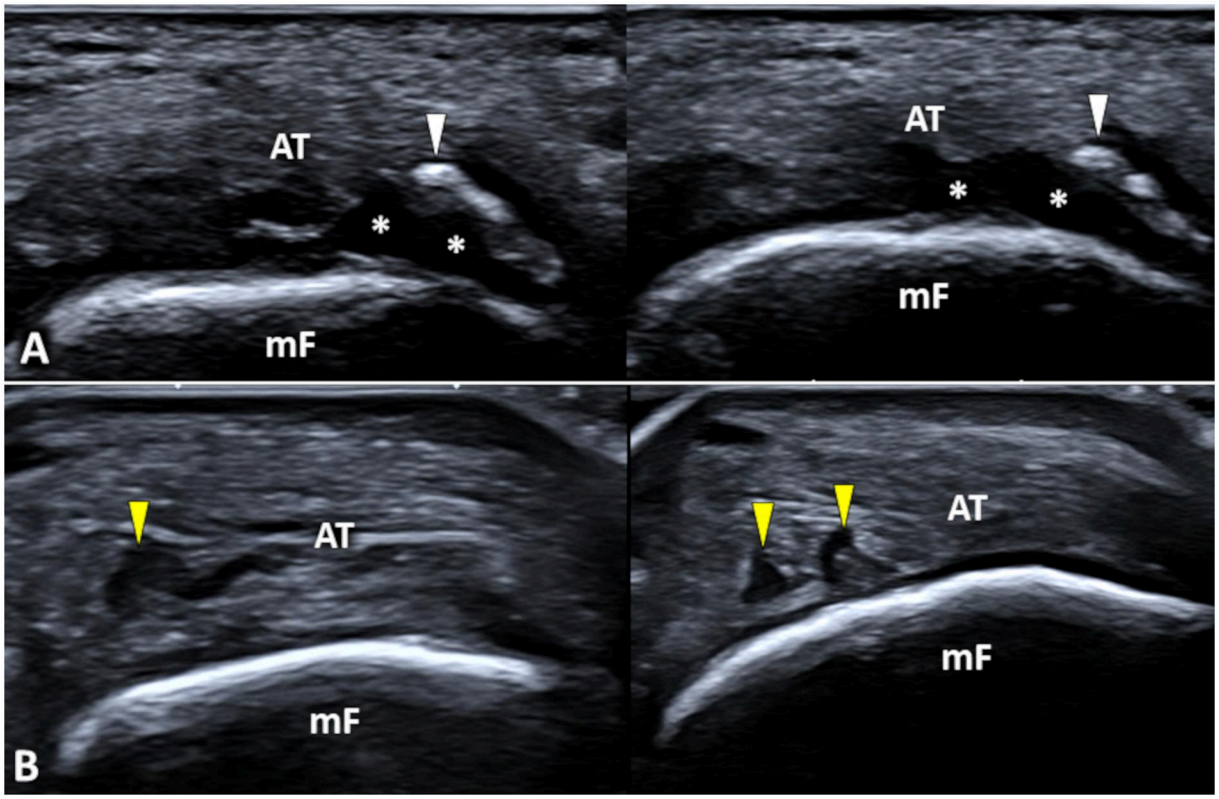

Figure 7. Transverse scans accurately differentiate the anechoic cartilaginous spur (*white asterisks*) with inner hyperechoic ossified foci (*white arrowhead*) (A) from the hypoechoic injuries (*yellow arrowheads*) involving the deep tendon fibres (B) at the level of the middle facet (*mF*) of the calcaneal tuberosity. Abbreviation: AT = Achilles tendon.

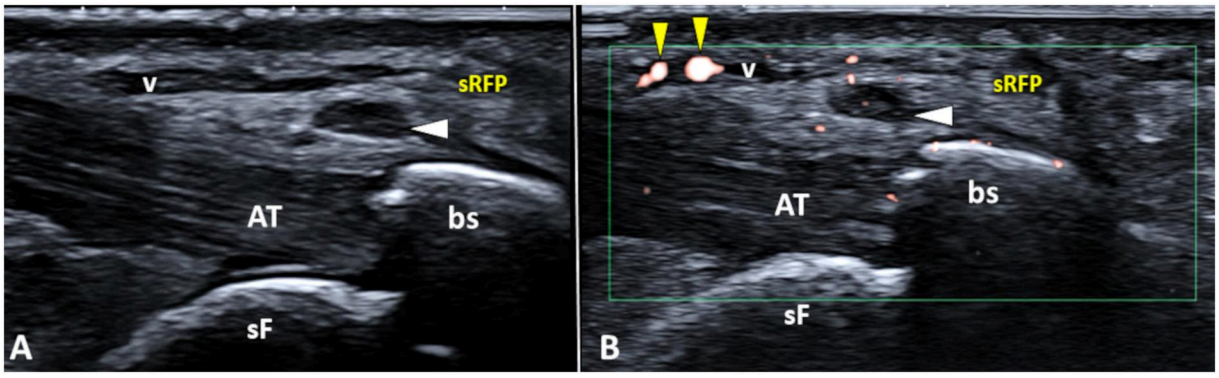

Figure 8. The superficial retrocalcaneal bursitis (*white arrowhead*) commonly appears as a hypoechoic nodular mass (A) between the bony spur (*bs*) of the calcaneal tuberosity and the superficial retrocalcaneal fat pad (*sRFP*)—without Doppler signals unlike the surrounding venous network (v) (B). Yellow arrowheads: vascular signals of the superficial venous network. Abbreviations: AT = Achilles tendon; sF = superior facet of the calcaneal tuberosity.

that is, hyperechoic cortical envelope with complete posterior acoustic shadowing, obscuring the underlying calcaneal tuberosity (Figure 10).[31,34] Dynamic US assessment of the ITBF (during active ankle dorsiflexion) can be performed to check for eventual impingement with the posterior surface of the calcaneus.[32]

The differential diagnosis between ITBF and intra-tendinous calcification of the AT can be challenging due to similar sonographic features. The former is usually larger than the calcification, whereby the colour/power Doppler does not reveal hypervascularization within the nearby tendon tissue. Instead, the intra-tendinous calcific deposition often shows intense hypervascularization of the adjacent tendon fibres in the acute/symptomatic phase (Video S7). Herein, the differential diagnosis between the 2 conditions is paramount for accurate management of IAT. Yet, ITBF does not reveal the evolving steps of softening and migration—described by Uhthoff for the hydroxyapatite deposition disease.[35-37]

In some patients, bone formation may not be detected within the tendon tissue but instead found between the AT, calcaneal tuberosity, and the Kager's fat pad. From proximal to distal, the bony fragment, superior facet, and the bony footprint of the AT can be observed as 3 different hyperechoic humps in long-axis view (Figure 10). The TZ connects the superior facet and the bony footprint of the AT. Herewith, the bony loose body is not in continuity with the

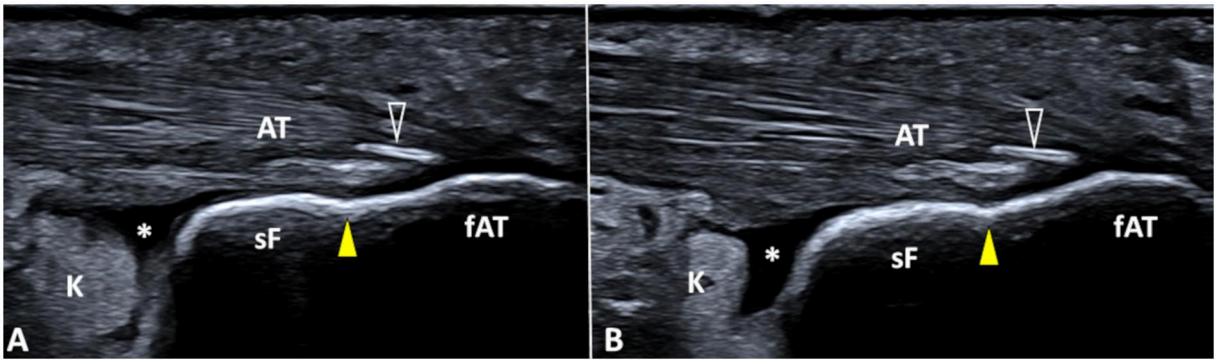

Figure 9. The calcified longitudinal fissuration of the tendon-bone junction of the Achilles tendon (AT) presents as a thin hyperechoic line (*void arrowhead*), aligned with the tendon fibres and without posterior acoustic shadowing (A). The transitional zone (*yellow arrowhead*) between the superior facet (sF) of the calcaneal tuberosity and the footprint of the AT (fAT) is preserved, and anechoic effusion (*white asterisk*) inside the deep retrocalcaneal bursa is visible (B). Abbreviation: K = Kager's fat pad.

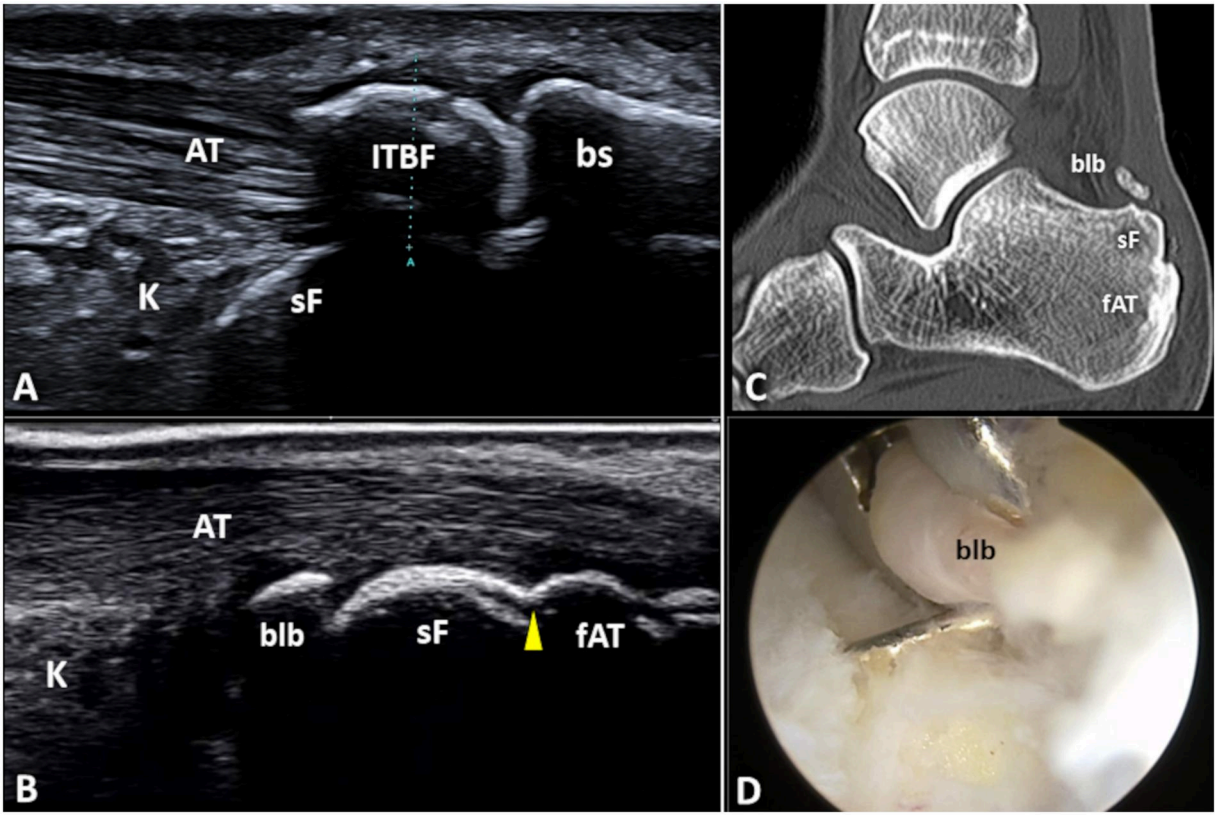

Figure 10. A massive bony spur (bs) combined with a large intra-tendinous bony formation (ITBF) makes the sonographic identification of the superior facet (sF) of the calcaneal tuberosity very challenging in this IAT patient (A). The 3 "humps" sonographic pattern (B) shows, from proximal to distal, the bony loose body (blb), the superior facet (sF) of the calcaneus, and the footprint of the AT (fAT). The CT (C) confirmed the bony loose body (blb) inside the deep retrocalcaneal bursa. Arthroscopic resection was performed to manage the posterior ankle impingement (D). Yellow arrowhead: transitional zone. Abbreviations: AT = Achilles tendon; K = Kager's fat pad.

cortex of the calcaneal tuberosity. Usually, the loose bone formation is located within the cavity of the deep retrocalcaneal bursa, potentially causing posterior impingement during ankle dorsiflexion.[38] Once again, the differential diagnosis between ITBF and the (intra-bursal) bony loose body is paramount because the latter often requires a surgical approach.

Tendon-bone disjunction

The transverse tears of the fibrocartilage plate, usually filled with fat cells and vascular connective tissue,[9,15,16] may progressively evolve to disinsertion of tendon fibres from the middle/inferior facet of the calcaneal tuberosity—that is, TBD. It may involve the most superficial fibres of the AT, forming a focal hypo/anechoic gap and proximal retraction of the tendon stump from the BS (Figure S11). Dynamic US scanning with active/passive ankle movements can be performed to stretch the tendon fibres and accurately confirm the abnormal motion, selectively involving the superficial fibres (Video S8).[32,33] Interestingly, colour/power Doppler assessment shows hypervascularization of the subcutaneous tissue-AT interface as an indirect sonographic sign of aberrant friction between the injured tendon fibres and the

surrounding soft tissues (Figure S11).[30] At this level, the gliding layer made of loose connective tissue is rich in vascular elements that penetrate and feed the most superficial fibres of the AT (Figure 4). In some patients, the differential diagnosis between TBD and focal tendinosis of the most distal fibres of the AT can be difficult. Colour/power Doppler can be used to confirm lack of vascular signals within the TBD—unlike insertional tendinosis which commonly shows intra-tendinous hypervascularization.[30]

TBD involving the AT deep fibres is hardly visible in the absence of anechoic effusion inside the deep retrocalcaneal bursa that acts as a natural contrast agent. Usually, it presents with a coarse sonographic pattern of the AT undersurface, just proximal to the superior facet of the calcaneal tuberosity, with blurred visibility of the classical fibrillar tendon pattern. Under US guidance, saline can be injected inside the bursal cavity to improve the sonographic visibility of TBD involving the AT undersurface. The anechoic fluid will penetrate within the injured tendon fibres, passing through the disrupted sesamoid fibrocartilage (Figure S12).[39] The procedure can be performed using an in-plane technique and a lateral-to-medial approach (Video S9). Thereafter, rotating the transducer 90°, the tendon stumps can be observed along its undersurface in long-axis view (Video S10).[40,41]

In some patients, the transverse micro-cracks of the fibrocartilage plate do not evolve in TBD, but they produce an irregular surface of the calcaneal tuberosity with multiple bone micro-pitting and thin trabeculae—forming the so-called "gnawed" pattern of the TBJ (Video S11).[42]

Fibrocartilage hyperemia

In the early phase of IAT, the TZ between the superior and middle facets of the calcaneal tuberosity is preserved, and the FCH usually presents a globular pattern involving the most distal portion of the TBJ of the AT (Figure S13). This sonographic pattern may be related to the histological and anatomical features of the most distal fibres of the AT that wrap the calcaneal tuberosity and are connected to the plantar fascia (via the periosteum). Indeed, they are more prone to mechanical stress due to their curved shape (Video S12).[21,22]

In the advanced stage of IAT, dysmorphic evolution of the middle and inferior facets with BS development, disappearance of the calcaneal TZ and massive hyperplasia of the microvasculature at the tendon attachment can be observed. Accurately setting the region of interest and the pulse repetition frequency for colour/power Doppler imaging,[43] vertically oriented donator vessels inside the fibrocartilaginous plate and horizontally oriented penetrating vessels insinuating among the tendon fibres can be identified (Figure S13). A similar sonographic pattern of FCH has been described at the lateral epicondyle of the elbow, with vascular ascending branches that originate from the hypoechoic cartilage of the enthesis and invading the tendon fibres.[5]

Neo-vessels are usually coupled with neo-nerves at the TBJ of the AT,[44,45] and detailed definition of the perfusion pattern is pivotal for specific US-guided procedures such as tendon perforation or fibrocartilage scraping (Table 2, Videos S13-S15).[46]

Conclusion

Using modern US equipment with high-frequency transducers, the "complex" anatomical structure of the TBJ of the AT can be thoroughly evaluated in IAT patients. The present standardized US protocol aims to define a common/technical language among musculoskeletal health care professionals. The above-described 5 elementary lesions comprise the main sonographic findings. Moreover, different US patterns for the BS (in the growing and end-stage phases) have been illustrated. The authors believe that this protocol can serve as a practical and ready-to-use guide in daily clinical practice while dealing with IAT patients.

Table 2. US-guided treatment of insertional Achilles tendinopathy.

Procedure	Technical note
Hydro-dissection	High-volume injection of the histological interface between the subcutaneous tissue and the posterior surface of the Achilles tendon to release the local adhesions involving the superficial retrocalcaneal bursae (Video S13)
Perforation	Multiple back-and-forward movements of the needle to fenestrate the fibrocartilaginous tissue of the tendon-bone junction and promote micro-bleedings and healing (Video S14)
Debridement	Multiple fan-shaped movements of the needle to remove fibrovascular scar tissue from the pathological tendon-bone junction (Video S15)

Acknowledgements

The pictures of the anatomic specimens were elaborated using donated bodies with the approval of the Institute of Anatomy, First Faculty of Medicine, Charles University, Prague. The authors sincerely thank those who donated their bodies to science so that anatomical research could be performed. Results from such research can potentially increase mankind's overall knowledge would improve patient care. Therefore, these donors and their families deserve our highest gratitude. The fetal microscopic specimen is a part of Doskočil's collection belonging to the same institution. These fetal models were prepared between the 1960s and 1970s in compliance with respective effective norms. The histological specimens used for the present investigation in Figure 1 were elaborated with the courtesy of the DIAP-Dipartimento InterAziendale di Anatomia Patologica di Bologna, Maggiore Hospital-AUSL Bologna, Bologna, Italy; and the Department of Medical and Surgical Sciences (DIMEC), University of Bologna, Bologna, Italy.

Author contributions

Giulio Cocco and Levent Özçakar contributed equally to this work and shared the senior authorship.

Vincenzo Ricci (Conceptualization), Vincenzo Ricci, Giulio Cocco, Costantino Ricci, Ondřej Naňka (Writing—original draft preparation), Toru Omodani, Ke-Vin Chang, Massimo Caulo, Vito Cantisani, Levent Özçakar (Writing—review and editing), Antonio Corvino, Andrea Delli Pizzi, Giorgio Tamborrini, Levent Özçakar (Supervision). All authors have read and agreed to the published version of the manuscript.

Supplementary material

Supplementary material is available at *BJR* online.

Funding

This study was supported by the Cooperatio Project Morphological Disciplines of Medicine, Charles University.

Conflicts of interest

M.C. is a Deputy Editor of the journal.

Ethical statement

All data reported in the present investigation were routine ultrasound imaging examinations, and there was no clinical intervention for the participants in the study.

Informed consent

Informed consent was obtained from all participants for routine ultrasound imaging examinations. However, due to the retrospective design of this study, the requirement for informed consent to participate in the study was waived by the Institutional Review Board.

References

1. Krishna Sayana M, Maffulli N. Insertional achilles tendinopathy. *Foot Ankle Clin*. 2005;10:309-320. https://doi.org/10.1016/j.fcl.2005.01.010
2. van Dijk CN, van Sterkenburg MN, Wiegerinck JI, Karlsson J, Maffulli N. Terminology for achilles tendon related disorders. *Knee Surg Sports Traumatol Arthrosc*. 2011;19:835-841. https://doi.org/10.1007/s00167-010-1374-z
3. Shaw HM, Vázquez OT, McGonagle D, Bydder G, Santer RM, Benjamin M. Development of the human achilles tendon enthesis organ. *J Anat*. 2008;213:718-724. https://doi.org/10.1111/j.1469-7580.2008.00997.x
4. Theobald P, Bydder G, Dent C, Nokes L, Pugh N, Benjamin M. The functional anatomy of kager's fat pad in relation to retrocalcaneal problems and other hindfoot disorders. *J Anat*. 2006;208:91-97. https://doi.org/10.1111/j.1469-7580.2006.00510.x
5. Ricci V, Cocco G, Mezian K, et al. Anatomy and sonographic examination for lateral epicondylitis: EURO-MUSCULUS/USPRM approach. *Am J Phys Med Rehabil*. 2023;102:300-307. https://doi.org/10.1097/PHM.0000000000002090
6. Ricci V, Tamborrini G, Zunica F, et al. High-resolution ultrasound imaging of elementary lesions in dactylitis. *J Ultrasound*. 2024;27:281-290. https://doi.org/10.1007/s40477-023-00834-z
7. Balint PV, Terslev L, Aegerter P, et al.; OMERACT Ultrasound Task Force Members. Reliability of a consensus-based ultrasound definition and scoring for enthesitis in spondyloarthritis and psoriatic arthritis: an OMERACT US initiative. *Ann Rheum Dis*. 2018;77:1730-1735. https://doi.org/10.1136/annrheumdis-2018-213609
8. Terslev L, Naredo E, Iagnocco A, et al.; Outcome Measures in Rheumatology Ultrasound Task Force. Defining enthesitis in spondyloarthritis by ultrasound: results of a delphi process and of a reliability reading exercise. *Arthritis Care Res (Hoboken)*. 2014;66:741-748. https://doi.org/10.1002/acr.22191
9. Rufai A, Ralphs JR, Benjamin M. Structure and histopathology of the insertional region of the human achilles tendon. *J Orthop Res*. 1995;13:585-593. https://doi.org/10.1002/jor.1100130414
10. Benjamin M, Kumai T, Milz S, Boszczyk BM, Boszczyk AA, Ralphs JR. The skeletal attachment of tendons—tendon "entheses". *Comp Biochem Physiol A Mol Integr Physiol*. 2002;133:931-945. https://doi.org/10.1016/s1095-6433(02)00138-1
11. Kuettner KE, Kimura JH. Proteoglycans: an overview. *J Cell Biochem*. 1985;27:327-336. https://doi.org/10.1002/jcb.240270403
12. Rossetti L, Kuntz LA, Kunold E, et al. The microstructure and micromechanics of the tendon-bone insertion. *Nat Mater*. 2017;16:664-670. https://doi.org/10.1038/nmat4863
13. Thorpe CT, Birch HL, Clegg PD, Screen HR. The role of the non-collagenous matrix in tendon function. *Int J Exp Pathol*. 2013;94:248-259. https://doi.org/10.1111/iep.12027
14. Rigozzi S, Müller R, Stemmer A, Snedeker JG. Tendon glycosaminoglycan proteoglycan sidechains promote collagen fibril sliding-AFM observations at the nanoscale. *J Biomech*. 2013;46:813-818. https://doi.org/10.1016/j.jbiomech.2012.11.017
15. Benjamin M, Rufai A, Ralphs JR. The mechanism of formation of bony spurs (enthesophytes) in the achilles tendon. *Arthritis Rheum*. 2000;43:576-583. https://doi.org/10.1002/1529-0131(200003)43:3<576::AID-ANR14>3.0.CO;2-A
16. Benjamin M, Toumi H, Suzuki D, Hayashi K, McGonagle D. Evidence for a distinctive pattern of bone formation in enthesophytes. *Ann Rheum Dis*. 2009;68:1003-1010. https://doi.org/10.1136/ard.2008.091074
17. Ballal MS, Walker CR, Molloy AP. The anatomical footprint of the achilles tendon: a cadaveric study. *Bone Joint J*. 2014;96-B:1344-1348. https://doi.org/10.1302/0301-620X.96B10.33771 PMID: 25274919.
18. Edama M, Kubo M, Onishi H, et al. Structure of the achilles tendon at the insertion on the calcaneal tuberosity. *J Anat*. 2016;229:610-614. https://doi.org/10.1111/joa.12514
19. Kachlik D, Baca V, Cepelik M, Hajek P, Mandys V, Musil V. Clinical anatomy of the calcaneal tuberosity. *Ann Anat*. 2008;190:284-291. https://doi.org/10.1016/j.aanat.2008.02.001
20. Szaro P, Witkowski G, Smigielski R, Krajewski P, Ciszek B. Fascicles of the adult human achilles tendon—an anatomical study. *Ann Anat*. 2009;191:586-593. https://doi.org/10.1016/j.aanat.2009.07.006
21. Snow SW, Bohne WH, DiCarlo E, Chang VK. Anatomy of the achilles tendon and plantar fascia in relation to the calcaneus in various age groups. *Foot Ankle Int*. 1995;16:418-421. https://doi.org/10.1177/107110079501600707
22. Singh A, Zwirner J, Templer F, Kieser D, Klima S, Hammer N. On the morphological relations of the achilles tendon and plantar fascia via the calcaneus: a cadaveric study. *Sci Rep*. 2021;11:5986. https://doi.org/10.1038/s41598-021-85251-0
23. Doral MN, Alam M, Bozkurt M, et al. Functional anatomy of the achilles tendon. *Knee Surg Sports Traumatol Arthrosc*. 2010;18:638-643. https://doi.org/10.1007/s00167-010-1083-7
24. Lohrer H, Arentz S, Nauck T, Dorn-Lange NV, Konerding MA. The achilles tendon insertion is crescent-shaped: an in vitro anatomic investigation. *Clin Orthop Relat Res*. 2008;466:2230-2237. https://doi.org/10.1007/s11999-008-0298-0
25. Mahan J, Damodar D, Trapana E, et al. Achilles tendon complex: the anatomy of its insertional footprint on the calcaneus and clinical implications. *J Orthop*. 2020;17:221-227. https://doi.org/10.1016/j.jor.2019.06.008
26. Ricci V, Chang KV, Naňka O, Özçakar L. Superficial retrocalcaneal bursae and nerves: from anatomy to ultrasound-guided procedures. *Clin Anat*. 2025;38:29-34. https://doi.org/10.1002/ca.24193
27. Williams, P.L., eds. Gray's Anatomy. 38th ed. *Churchill Livingstone*; 1995: 886 pp.
28. Lindén L, Granath M, Hedlund P, Spang C, Alfredson H. Ultrasonography- and Doppler-Guided surgical treatment for insertional achilles tendinopathy: results from a case series in a Southern Sweden county hospital. *Foot Ankle Orthop*. 2023;8:24730114231165014. https://doi.org/10.1177/24730114231165014
29. Chimenti RL, Chimenti PC, Buckley MR, Houck JR, Flemister AS. Utility of ultrasound for imaging osteophytes in patients with insertional achilles tendinopathy. *Arch Phys Med Rehabil*. 2016;97:1206-1209. https://doi.org/10.1016/j.apmr.2015.12.009
30. Cocco G, Ricci V, Corvino A, et al. Musculoskeletal disorders in padel: from biomechanics to sonography. *J Ultrasound*. 2024;27:

335-354. https://doi.org/10.1007/s40477-023-00869-2 Epub 2024 Apr 5. PMID: 38578364.
31. Cocco G, Ricci V, Villani M, et al. Ultrasound imaging of bone fractures. *Insights Imaging*. 2022;13:189. https://doi.org/10.1186/s13244-022-01335-z
32. Pirri C, Stecco C, Güvener O, et al.; EURO-MUSCULUS: European Musculoskeletal Ultrasound Study Group in Physical and Rehabilitation Medicine. EURO-MUSCULUS/USPRM dynamic ultrasound protocols for ankle/foot. *Am J Phys Med Rehabil*. 2024;103:e29-e34. https://doi.org/10.1097/PHM.0000000000002349
33. Cocco G, Ricci V. Dynamic ultrasound assessment for insertional achilles tendinopathy: the COcco-RIcci (CORI) sign. *Skeletal Radiol*. 2025;54:593-599. https://doi.org/10.1007/s00256-024-04746-9
34. Ricci V, Soylu AR, Özçakar L. Artifacts and artistic facts: a visual simulation for ultrasound training. *Am J Phys Med Rehabil*. 2019;98:521-525. https://doi.org/10.1097/PHM.0000000000001134
35. Uhthoff HK, Sarkar K. Calcifying tendinitis. *Baillieres Clin Rheumatol*. 1989;3:567-581. https://doi.org/10.1016/s0950-3579(89)80009-3
36. Uhthoff HK, Loehr JW. Calcific tendinopathy of the rotator cuff: pathogenesis, diagnosis, and management. *J Am Acad Orthop Surg*. 1997;5:183-191. https://doi.org/10.5435/00124635-199707000-00001
37. Ricci V, Mezian K, Chang KV, Özçakar L. Clinical/sonographic assessment and management of calcific tendinopathy of the shoulder: a narrative review. *Diagnostics (Basel)*. 2022;12:3097. https://doi.org/10.3390/diagnostics12123097.
38. Ricci V, Cocco G, Mezian K, et al. Histo-anatomy and sonographic examination for the retrocalcaneal bursal complex: EURO-MUSCULUS/USPRM approach. *J Ultrasound Med*. 2024;43:2027-2038. https://doi.org/10.1002/jum.16544
39. Ricci V, Özçakar L. Life after ultrasound: are we speaking the same (or a new) language in physical and rehabilitation medicine? *J Rehabil Med*. 2019;51:234-235. https://doi.org/10.2340/16501977-2527
40. Albano D, Messina C, Gitto S, Serpi F, Sconfienza LM. Imaging-guided musculoskeletal interventions in the lower limb. *Radiol Clin North Am*. 2023;61:393-404. https://doi.org/10.1016/j.rcl.2022.10.012
41. Sconfienza LM, Adriaensen M, Albano D, et al. Clinical indications for image-guided interventional procedures in the musculoskeletal system: a Delphi-based consensus paper from the european society of musculoskeletal radiology (ESSR)-part VI, foot and ankle. *Eur Radiol*. 2022;32:1384-1394. https://doi.org/10.1007/s00330-021-08125-z
42. Fodor D, Rodriguez-Garcia SC, Cantisani V, et al. The EFSUMB guidelines and recommendations for musculoskeletal ultrasound—part I: extraarticular pathologies. *Ultraschall Med*. 2022;43:34-57. https://doi.org/10.1055/a-1562-1455
43. Ricci V, Ricci C, Tamborrini G, et al. From histology to sonography in synovitis: EURO-MUSCULUS/USPRM approach. *Pathol Res Pract*. 2023;241:154273. https://doi.org/10.1016/j.prp.2022.154273
44. De Lorenzis E, Natalello G, Simon D, Schett G, D'Agostino MA. Concepts of entheseal pain. *Arthritis Rheumatol*. 2023;75:493-498. https://doi.org/10.1002/art.42299
45. Bring DK, Heidgren ML, Kreicbergs A, Ackermann PW. Increase in sensory neuropeptides surrounding the achilles tendon in rats with adjuvant arthritis. *J Orthop Res*. 2005;23:294-301. https://doi.org/10.1016/j.orthres.2004.08.017
46. Ricci V, Mezian K, Cocco G, et al. Ultrasonography for injecting (around) the lateral epicondyle: EURO-MUSCULUS/USPRM perspective. *Diagnostics (Basel)*. 2023;13:717. https://doi.org/10.3390/diagnostics13040717

British Journal of Radiology, 2026, 99, 122–132
https://doi.org/10.1093/bjr/tqaf231
Research Article